Journal of
Materials Chemistry B

Accepted Manuscript

ROYAL SOCIETY OF CHEMISTRY

www.rsc.org/materialsB

Electrochemical deposition to construct nature inspired multilayer chitosan/layered double hydroxides hybrid gel for stimuli responsive release of protein

Pengkun Zhao, Youyu Liu, Ling Xiao, Hongbing Deng, Yumin Du, Xiaowen Shi*

School of Resource and Environmental Science and Hubei Biomass-Resource Chemistry and Environmental Biotechnology Key Laboratory, Wuhan University, Wuhan 430079, China

E-mail: shixwwhu@163.com; Tel: +86-27-68778501

Abstract

In this study, we report a single electrodeposition process to fabricate multilayered chitosan/layered double hydroxides (LDHs) hybrid hydrogel for stimuli responsive protein release. LDHs nanoplatelets with regular hexagonal shape were synthesized by hydrothermal method and a model protein, insulin, was adsorbed to the surface of LDHs (INS-LDHs) caused by electrostatic interactions. The insulin loading ratio could reach 20% (w/w) and the INS-LDHs were characterized by energy dispersive spectrometer (EDS), Fourier transform infrared spectroscopy (FT-IR), thermogravimetric analysis (TG) and zeta potential measurements. Co-electrodeposition of chitosan and INS-LDHs generated an inorganic and organic composite hydrogel with multilayered structure, as revealed by scanning electron microscopy (SEM). The hybrid hydrogel dramatically reduced the burst release of insulin from INS-LDHs. Significantly, the release of insulin was sensitive to the presence of anions, pHs and external potentials. Our results suggest that co-electrodeposition of stimuli-responsive polymer and nanoplatelets is an alternative and facile method to construct hierarchically structured hybrid hydrogel and the great potential of the multilayered structure in drug delivery.

Key words: Controlled drug release, Electrodeposition, Layered double hydroxides, Multi-sensitive chitosan hydrogel

1. Introduction

Nature has created many intriguing structures that demonstrate exceptional biological or mechanical properties and functionalities. Thus, people devote enormous efforts to mimicking the structure from the nature and have produced many materials having similar or even better

performance to natural products[1-3]. The brick-and-mortar construction in nacre and bone is a highly oriented layered structure made from organic and platelet inorganic components[4, 5]. Until now, there are enormous studies on mimicking this layered hybrid structure[4, 6]. However, most of the contributions focus on improving mechanical properties. The discovery of new applications in diverse field is meaningful for better understanding of this nature inspired structure.

A commonly used bottom-up method to build multilayered hybrid structure is layer-by-layer (LBL), which is efficient but time consuming[7]. Recent report on electrophoretic deposition (EPD) demonstrates that the nanoplatelets can be oriented to aligned structure under electric field[8]. EPD is a rapid and scalable process that can simultaneously assemble positively charged nanoplatelets and cationic polyelectrolytes[9]. As far as we know, the co-deposition of stimuli-responsive natural polymers and nanoplatelets to fabricate multilayered structure has never been reported. In addition, the stimuli drug release behavior from the brick-and-mortar structure is not well investigated. Thus, in this paper, we construct the layered structure by electrodeposition method and investigate the drug release behavior responding to external stimuli.

Chitosan is a unique cationic polysaccharide containing amino groups and having important applications in drug delivery, biomedicine and tissue engineering[10, 11]. It shows pH responsive sol-gel transition and can be deposited as a hydrogel on electrode when biasing a negative potential. The *in situ* sol-gel transition is induced by an increased pH gradient due to the consumption of protons at the cathode[11, 12]. By co-depositing chitosan and nanocomponents, organic and inorganic hybrid hydrogel can be facilely obtained on the surface of the cathode, which has demonstrated important applications in electrical analysis, biosensor and protein assembly[13, 14]. Herein, we co-deposit chitosan and a kind of nanoplatelet, layered double hydroxides (LDHs), to generate multilayered structure that mimics the natural brick-and-mortar structure.

LDHs are a class of octahedral ionic lamellar compounds, having positively charged metal hydroxide layer and compensating anions. It has the general formula

$[M^{2+}_{1-x}M^{3+}_{x}(OH)_2]^{x+}[A^{n-}_{x/n}]^{x-}\cdot mH_2O$ (where M^{2+} and M^{3+} are divalent and trivalent metals, respectively, and A^{n-} is the interlayer anion)[15]. LDHs nanoplatelets possess excellent anion exchange ability and a number of advantageous properties, such as good biocompatibility, low cytotoxicity, uniform morphologies and sizes, chemical and thermal stabilities, large surface-to-volume ratio and strong adsorption ability[16]. These inherent properties enable LDHs to carry anionic biomolecules such as DNAs[17], RNAs[18] and drugs[18-20]. In addition, there are studies about adsorption of proteins to LDHs' surface owing to its inherent positive charge[21]. However, most guest molecules release quickly from LDHs due to the large edge to volume ratio of the LDHs[22].

In this work, we co-electrodeposited chitosan and LDHs to generate multilayered structure for stimuli sensitive protein release. The layered hybrid structure would provide a long pathway for the protein to diffuse out and thus reduce the burst release[22]. Insulin was selected as a model protein. Diabetic patients usually need exogenous insulin and suffer from daily injection[23]. It is necessary to develop on demand insulin delivery systems that can release insulin according to surrounding stimuli, such as the presence of glucose[24], electrical potentials[25], pH changes[26, 27], light[28], magnetic field[29], temperature changes[30] and ultrasound[31]. We demonstrate insulin release from the hybrid chitosan and INS-LDH hydrogel can be responsive to pH, anion and electrical signals. Scheme 1 illustrates our experimental procedure. The hexagonal shaped LDHs were hydrothermally synthesized for insulin loading. The insulin loaded LDHs (INS-LDHs) were dispersed in chitosan solution (pH 5) and co-deposited with chitosan hydrogel on a titanium plate by biasing a cathodic potential. The EPD of chitosan chain and INS-LDHs generated a hybrid hydrogel with multilayered structure, where the oriented LDHs were glued by chitosan. The release of insulin from the hydrogel was triggered by external stimuli, i.e. anions, pH changes or external potentials. This fast and simple EPD method to fabricate multilayered hybrid hydrogel and stimuli controlled drug release should expand the application of multilayered structure in drug-delivery system.

2. Experimental

2.1. Materials

Chitosan with a deacetylation degree of 85% and a molecular weight of 200 kDa was purchased from Sigma and provided as a coarse powder. Insulin (from bovine) was purchased from Sigma with a molecular weight of 5733.49 Da. Titanium plates with a thickness of 100 μm were purchased from Baoji Titanium Company, Shanxi. Magnesium chloride and aluminum chloride were purchased from Shanghai Reagent Co., Ltd (China). All reagents were of analytical grade and were used without further purification.

2.2. Preparation of layered double hydroxides

Layered double hydroxides, $Mg_2Al(OH)_6Cl{\cdot}xH_2O$ (Cl-LDHs), were prepared by a co-precipitation method in the presence of excess Mg^{2+} according to previously reported work with some modifications[32]. Briefly, $MgCl_2$ (2.28 g) and $AlCl_3$ (1.06 g) were dissolved in 80 ml water. Then the mixed salt solution was added within 5s to 320 ml NaOH solution (0.15 M) under vigorous stirring, followed by 15 min stirring isolated from air. The precursor was collected by centrifugation (9000 rpm for 5min) and washed twice. Then the precipitate was dispersed in 140 ml deionized water and hydrothermally treated in an autoclave at 100 °C for 18 h. The LDH crystallites were obtained via centrifugation (16000 rpm for 5min) and washed twice, then freeze-dried overnight for the following characterizations and protein loading. LDHs with anions of NO_3^- and CO_3^{2-} were also synthesized by hydrothermal method (detailed procedure was provided in supporting information).

2.3. Insulin loading on layered double hydroxides

In order to load insulin on LDHs, 0.25 g as-prepared LDHs were added to 50ml glycine-NaOH buffer solution (pH 8.6) containing 1.25 mg/ml insulin and stirred for 5h at room temperature until the absorption reached equilibrium. Then the INS-LDHs were obtained by centrifugation (16000 rpm for 5 min) and washed with glycine-NaOH buffer twice and freeze-dried overnight. The concentration of insulin in the supernatant was determined via UV absorption at 280nm, followed by calibration with an insulin standard curve. The difference between the amount of insulin initially introduced and the protein content in the supernatant is taken as an indication of the amount of insulin entrapped.

The insulin loading capacity (LC) of INS-LDHs was defined as follows:

$$\mathrm{LC} = \frac{\mathrm{M1} - \mathrm{M2}}{\mathrm{M1} - \mathrm{M2} + \mathrm{M3}} \times 100\%$$

where M1 is the mass of insulin initially introduced, M2 is the mass of insulin in the supernatant, M3 is the mass of LDHs initially introduced.

2.4. Electrodeposition of multilayered chitosan/INS-LDHs hydrogel

Briefly, chitosan solution was prepared by dissolving chitosan flakes in HCl solution (pH 3) under vigorous stirring and the undissolved flakes were removed by filtration. Before electrodeposition, the pH of the chitosan solution was adjusted to 5 by adding 1mol/L NaOH and NaCl was added to a final concentration of 0.25% (w/v). Then a certain amount of INS-LDHs was dispersed in 15 ml chitosan solution (1%, w/w) based on the mass ratio of chitosan to LDHs (3:1 to 1:2) and stirred for 30 min to get a homogeneous mixture. A titanium plate with a dimension of 4 cm × 2 cm × 100 μm was selected as the cathode for co-electrodeposition and cleaned by acetone, alcohol and water consecutively under sonication for 5 min each before deposition. The electrodeposition was carried out as follows: the titanium plate and a platinum wire were partially dipped into chitosan solution (1%, w/v) and the distance between the two electrodes was kept at 1 cm. A constant current (−0.75 mA/cm^2) was applied to the two electrodes for 30 min. The typical voltage for deposition was 3–4 V and the deposited hydrogel had a thickness of 2 mm. Then the white hydrogel on the titanium plate was rinsed briefly with distilled water. The amount of INS-LDHs entrapped in chitosan hydrogel was determined by dissolving hydrogel in pH 1.2 HCl solution, followed by centrifugation. The concentration of insulin in HCl solution was measured by its absorbance at 280nm as described above.

2.5. Anion responsive release of insulin from INS-LDHs and chitosan/INS-LDHs hydrogel

The release of insulin from INS-LDHs was performed in pH 9.0 solution containing 100 mM HPO_4^{2-}, SO_4^{2-}, CO_3^{2-}, Cl^- or NO_3^- respectively. The release was also carried out in 1 mM, 5 mM or 10 mM phosphate buffer at pH 7.4. Typically, 0.15 g INS-LDHs were added in 50 ml colorimetric tube which contained above solutions at 37°C. At predetermined time intervals, 5 ml of the release medium was withdrawn and centrifuged at 16000 rpm for 5 min. The insulin concentration in the

supernatant was analyzed by UV–vis spectroscopy. Each assay was carried out in triplicate.

The release of insulin from INS-LDHs hydrogel was carried out in a similar way. The electrodeposited hydrogel was immersed in 20 ml solution and the released insulin was measured by UV-vis. In some cases, the release buffer contained 0.1 M NO_3^-, Cl^-, or SO_4^{2-} and the pH of the solution varied at 4.0, 7.0 or 9.0. Each assay was also carried out in triplicate.

2.6. Electrochemically controlled insulin release from chitosan/INS-LDHs hydrogel

A titanium plate with deposited chitosan/INS-LDHs hydrogel was partially immersed in 0.9% NaCl solution and a platinum wire worked as counter electrode. The release of insulin was activated by applying a voltage of 0 V, 5 V or −5 V respectively. In the case of 0 V, 0.9% NaCl solutions with different pHs (4.0, 7.0, 9.0) were used as the release medium. In the on-off mode, the time sequence of the voltage was “on” for 30 min and “off” for 30 min, and the voltage was set as +5V or -5V. The release of insulin was monitored by UV–vis method described above. Each assay was also carried out in triplicate.

2.7. Characterization of LDHs, INS-LDHs and chitosan/INS-LDHs

Transmission electron microscopy (TEM) was performed using a JEM-100CXII. The field emission scanning electron microscopy (FE-SEM, ZEISS, Germany) was applied to observe the morphology of the LDHs and chitosan/INS-LDHs hydrogel. The size distribution and zeta potential of LDHs and INS-LDHs were determined by zetasizer 3690 (Malvern, UK). LDHs were dispersed in water and sonicated for 5 min before measurement. The distribution of ions at the surface of INS-LDHs was measured by Energy Dispersive Spectrometer (EDS, XSAM800). X-ray diffraction (XRD) tests were carried out on a XRD diffractometer (D8-Advance, Bruker). The XRD patterns with Cu K_α radiation (0.154 nm) at 40 kV and 40 mA were recorded in 2θ range of 7–80°. Samples for Fourier transform infrared spectra (FT-IR) were vacuum dried overnight at 60°C and recorded using KBr pellet method on a Nicolet 5700 Fourier transform infrared spectrometer. Thermal behaviors of samples were examined by thermogravimetric analysis (TGA, Shimadzu DTG-60) at room temperature up to 600°C at a heating ramp of 5°C min^{-1}. The absorbance at 280 nm for released insulin was measured by UV spectrophotometer (UV-1780, Shimadzu).

3. Results and discussion

Cl-LDHs were prepared by a co-precipitation method in the presence of excess Mg^{2+} [32]. The precursors (Mg-OH and Al-OH) for LDH synthesis were hydrothermally treated for 18 h at 100 ^{o}C. The SEM and TEM images of Cl-LDHs were shown in Fig.1. Cl-LDHs have well defined hexagonal shape and the lateral size is in the range of 60-150 nm. From TEM images, some single LDH plates can be found, which can enlarge the surface area and facilitate further protein loading. The SEM images of LDHs with anions of NO_3^- and CO_3^{2-} (NO_3-LDHs and CO_3-LDHs) exhibit aggregated sheets and particles (Fig.S1). Further, the insulin loading amount of CO_3-LDHs and NO_3-LDHs is lower than that of Cl-LDHs. Therefore, we use Cl-LDHs for insulin loading and hydrogel formation in the following study.

Next insulin was loaded on LDH plates by incubating LDHs in glycine-NaOH buffer (pH 8.6) containing insulin for 5 h. The residue of insulin was removed by washing with glycine-NaOH buffer solution twice. The Energy Dispersive Spectrometer (EDS) gives the evidence for insulin loading on LDHs (Fig.2). There are mainly four elements (Mg, Al, O, Cl) on the surface of pristine LDHs (Fig.2A). Elemental analysis gives the atomic ratio [Mg]/[Al]=1.7-1.8, slightly less than the designed value (2.0), which is due to more Mg^{2+} leaching than Al^{3+} from the hydroxide layers[33, 34]. After the insulin loading (Fig.2B), the appearance of C, N and S peaks give the evidence that insulin was loaded on the surface of LDHs. The change of size distribution of LDHs before and after insulin loading was measured by Malvern laser particle size analyzer. The average hydrodynamic diameter of pristine LDHs dispersed in water is 68 nm, as shown in Fig.2C, which is in accordance with the SEM and TEM analysis. The insulin loaded LDHs (Fig.2D) show similar size distribution curves compared to pristine LDHs, indicating that insulin loading did not change the diameter of LDHs.

However, the loading of insulin remarkably affected the surface charge of LDHs. The LDHs had a zeta-potential of 8.62 mV at pH 7, which changed to -4.2 mV after the adsorption of insulin (Table.1). The insulin molecule (pI 5.3-5.4) contains negative charge residues, for instance, aspartic acid and glutamic acid, showing a net charge of -19mV at neutral pH. These residues

would be attracted by the LDHs surface, resulting in INS-LDHs with more negative charge because of charge compensation. This suggests that the insulin molecules exhibit electrostatic affinity for the LDHs surface and thus change the potential of the electrical double layer of the LDH nanoplatelets[14, 35, 36].

The X-ray diffraction patterns of the pristine LDHs and INS-LDHs were shown in Fig.3A. LDHs exhibited series of $00l$ Bragg reflections which are the characteristic reflections of the LDHs layered structure. In the XRD pattern of INS-LDHs, the (003), (006) and (009) peaks didn't show noticeable shift. Further, the basal spacing (d_{003}) of the pristine LDHs is 0.77 nm which is identical with the INS-LDHs[37]. Considering the size of insulin molecule is in the range of several nanometers, it is reasonable to conclude that no intercalation of LDHs by insulin has occurred, and insulin was mainly adsorbed on the surface of LDHs.

Further evidence of insulin loading on LDHs was provided by FT-IR spectroscopy (Fig.3B). In the FT-IR curve of pure insulin, absorption bands were detected at wavelengths 1652 cm^{-1} and 1544 cm^{-1}. These bands were related to the functional groups found in insulin: amide I (protein C=O stretching) and amide II (protein N–H bend, C–N stretch), respectively[38]. In the spectrum of LDHs, a broad absorption band at around 3500cm^{-1} was attributed to OH stretching due to the presence of hydroxyl groups on LDHs. The absorbance at 1627cm^{-1} was assigned to the bending vibrations of the interlayer water molecules[33]. Although the reactions were performed under N_2 atmosphere, the strong absorbance at 1360cm^{-1} indicated the existence of small amount of CO_3^{2-}, which was due to unavoidable absorption of CO_2 by the basic solution[39]. In the FT-IR spectrum of INS-LDHs, the retention of the peaks at 1652 cm^{-1} and 1544 cm^{-1} which were the characteristic peaks of insulin (amide I and amide II) and the peaks at 3500 cm^{-1} and 1360 cm^{-1} which were originated from LDHs gives further evidence that insulin was loaded on LDHs.

Fig.3C displayed the TG curves of insulin, LDHs and INS-LDHs. For insulin, the initial weight loss at 100 ^{o}C was caused by water evaporation and the loss at 225 ^{o}C was associated with insulin decomposition. LDHs showed a weight loss started at 60 ^{o}C owing to the loss of adsorbed and interlayer water. From 370 ^{o}C to 600 ^{o}C, the weight loss was mainly due to the dehydroxylation of

the LDH sheets[40]. The onset of degradation temperature (235 ^{o}C) of INS-LDHs is obviously lower than that of LDHs (370 ^{o}C), due to the presence of insulin in INS-LDHs. Because insulin is physically adsorbed to LDHs, the degradation temperature of INS-LDHs is close to that of insulin. The degree of weight loss during thermal analysis correlated closely with the amount of insulin loaded in LDHs. Based on the weight loss ratios of insulin, LDHs and INS-LDHs, it can be estimated that the weight percentage of insulin in INS-LDHs is about 21%. By analyzing the difference between the amount of insulin initially introduced and the protein content in the supernatant, the insulin loading capacity (LC) was calculated to be 20.3%, which is comparable to the TG analysis.

Since the electrostatic interaction plays an important role for insulin loading, the anions may have a profound effect on insulin release. We monitored the release of insulin by incubating INS-LDHs in pH 9 buffer containing 0.1 M HPO_4^{2-}, SO_4^{2-}, CO_3^{2-}, Cl^- or NO_3^- respectively. From Fig.4A, burst release of insulin was observed in buffers containing SO_4^{2-}, CO_3^{2-}, HPO_4^{2-} and a relatively slow release in Cl^- and NO_3^-. This phenomenon can be explained by the different binding competence between divalent and monovalent anions[41]. The release rate was also related to the concentration of anions. As shown in Fig.4B, the release rate increased dramatically as the phosphate concentration increased, which is expected since high concentration phosphate ions have more opportunities to compete with Mg-sites and Al-sites.

The insulin release behavior can be adjusted by forming multilayered structure with chitosan hydrogel. Our previous work suggested that mesoporous silica nanoparticles can be co-deposited with chitosan hydrogel[11]. When chitosan and LDHs were co-deposited, the electric field could align the LDHs with positive surfaces paralleling to the electrode. This favorable parallel orientation was also observed for gibbsite nanoplatelets deposition under direct-current electric field[8]. During the deposition, the localized sol-gel transition of chitosan and the electrophoretic deposition of nanoplatelets built the multilayered structure. The optical and SEM images of the deposited hydrogel (chitosan to LDHs ratio 1:1) were shown in Fig.5. The pure chitosan hydrogel on titanium plate was transparent (Fig.5A) after deposition at –0.75 mA/cm^2 for 30 min, while the co-deposition of chitosan and INS-LDHs resulted in an opaque hydrogel (Fig.5D). The

cross-section of dried hydrogel was observed by using scanning electron microscopy (SEM). Compared to pure chitosan hydrogel (Fig.5B and 5C), the chitosan/INS-LDHs hydrogel (Fig.5E and 5F) revealed a multilayered structure. The enlarged image in Fig.5F clearly showed the aligned LDHs in chitosan hydrogel. Besides, SEM images of the hydrogels with other chitosan to INS-LDHs ratio (3:1 to 1:2) were provided in Fig.S2. The chitosan/LDHs films became more compact and less transparent with the increasing ratio of LDHs. In the case of chitosan to LDHs ratio of 1:1, the amount of INS-LDHs deposited per cm^2 in hydrogel could reach 2.5 mg/cm^2, however, for insulin that was 0.5 mg/cm^2.

The formation of multilayered chitosan/INS-LDHs hydrogel dramatically altered the release behavior of insulin. Firstly, the burst release of insulin, as demonstrated previously in Fig.4A, was obviously reduced. Chitosan/INS-LDHs hydrogel was immersed in 0.1 M NO_3^- solution with different pHs (4.0, 7.0 9.0). At pH 9.0, the release of insulin from INS-LDHs reached 10% at first 15 min and it was only 4% at 2 h for chitosan/INS-LDHs (Fig. 6A), indicating the multilayered structure retarded the protein release. Secondly, the release of insulin from chitosan/INS-LDHs was affected by surrounding pHs. The release at pH 4.0 and 9.0 was faster than that at pH 7.0. At pH 4.0, the electrostatic interactions between LDHs and insulin were reduced as well as the swelling of chitosan facilitated the release of insulin. The different release behavior between pH 7.0 and 9.0 could be explained by the low solubility of insulin in neutral pH. Thirdly, the release can be adjusted by the presence of various anions. At pH 9.0, the release of insulin in 0.1 M NO_3^- is 10%, while sequentially changing the release medium with CO_3^{2-} and SO_4^{2-} didn't reduce the release rate, due to the different abilities of anions to interact with Mg-sites and Al-sites. By comparison, the chitosan/INS-LDHs hydrogel was incubated in sole NO_3^- solution (0.1 M) at different pHs for 8 h. It was observed that the release rate of insulin decreased gradually and reached equilibrium after 4 h (the release curves were plotted by dotted lines).

Inspired by the stimuli responsive release of insulin from the chitosan/INS-LDHs hybrid hydrogel, electrical signals were used to regulate insulin release. The titanium plate with chitosan/INS-LDHs hydrogel was immersed in 0.9% NaCl solution and activated by applying a positive or negative potential. We first investigated the release behavior of insulin from INS-LDHs hydrogel in 0.9%

NaCl solution without applying a voltage but changing the pH as pH 4.0, pH 7.0 and pH 9.0. As indicated in Fig.S3, faster insulin release could be observed under pH 4.0 and pH 9.0. This observation is consistent with the results in Fig.6A, in which slow release was found at neutral pH. However, the electrical stimulus tremendously accelerated the release of insulin when compared to the release under unbiased potential (Fig.6B). During 12 h, the cumulative release increased from 4.9% to 36.5% under -5.0V and to 58.5% under +5.0 V. It was observed that the pH condition in chitosan/LDHs hydrogel shifted under the potential. The pH of the hydrogel could rise from 7 to 8~9 under -5.0V and decline to 4~5 under +5.0V. As discussed above, the change of pH environment in the hydrogel induced by applied potential adjusted the release behavior of insulin, leading to faster release than 0 V (pH 7.0). Therefore, electrical signals can be used to induce different release rate of insulin from the LDHs/chitosan hydrogel.

Finally, the release profile of insulin can be manipulated by switching the voltage as on-off mode. The applied voltage was programmed as “on” for 30 min and then “off” for 30 min. A pulsed release pattern can be realized responding to the imposed electrical signals, although the step-wised release is more obvious in the first 4 h (Fig.6C). It was worth to note that positive potential (+5.0V) has more profound influence than negative potential (-5.0V), which was in agreement with the result in Fig.6B. When comparing the on-off release with the continuous release, the on-step contributed significantly to the release of insulin, while the release in off-step is quite slow. The results suggest the release of insulin from chitosan/INS-LDHs hydrogel could be tuned by applying different voltages.

4. Conclusions

By simultaneously eletrodepositing chitosan and LDHs nanopletelets, a multilayered chitosan/LDHs hybrid hydrogel was facilely fabricated, mimicking the brick-and-mortar structure in nature. The pH responsive and film forming property of chitosan and positive change surface and nanoscale of LDHs allow the gradual layer structure construction under electric field. We explored the ability of the nature inspired multilayered hydrogel as an insulin controlled release platform. External stimulus, such as pH, anion, and electrical potential has a profound influence

on the release of insulin. Significantly, on demand insulin release can be realized by programming the exerting electrical potentials. The present results suggest the advantage of electrodeposition in the build of multilayered structure using stimuli-responsive natural polymers and nanocomponents as well as great potentials of the brick-and-mortar structure in controlled drug release.

Acknowledgements

This work was financially supported by National Natural Science Foundation of China (Grant nos. 51373124 and 21007049), "Youth Chen-Guang Project" of Wuhan Bureau of Science and Technology (2014070404010196) , Program for New Century Excellent Talents in University (NECT-10-0618) and Special Fund for Environmental Protection in the Public Interest (2013467064).

References

1. U. G. Wegst, H. Bai, E. Saiz, A. P. Tomsia and R. O. Ritchie, *Nature materials*, 2015, **1**, 23-36.
2. L. J. Bonderer, A. R. Studart and L. J. Gauckler, *Science*, 2008, **319**, 1069-1073.
3. A. R. Studart, *Advanced Materials*, 2012, **24**, 5024-5044.
4. S. Xia, Z. Wang, H. Chen, W. Fu, J. Wang, Z. Li and L. Jiang, *Acs Nano*, 2015, **9**, 2167-2172.
5. P. Y. Chen, A. Y. Lin, Y. S. Lin, Y. Seki, A. G. Stokes, J. Peyras, E. A. Olevsky, M. A. Meyers and J. Mckittrick, *Journal of the Mechanical Behavior of Biomedical Materials*, 2008, **1**, 208–226.
6. Y. Shu, P. Yin, J. Wang, B. Liang, H. Wang and L. Guo, *Ind.eng.chem.res*, 2014, **53**, 3820-3826.
7. W. Tong, X. Song and C. Gao, *Chemical Society Reviews*, 2012, **41**, 6103-6124.
8. T.-H. Lin, W.-H. Huang, I.-K. Jun and P. Jiang, *Chemistry of Materials*, 2009, **21**, 2039-2044.
9. T.-H. Lin, W.-H. Huang, I.-K. Jun and P. Jiang, *Electrochemistry Communications*, 2009, **11**, 1635-1638.
10. K. Yan, F. Ding, W. E. Bentley, H. Deng, Y. Du, G. F. Payne and X.-W. Shi, *Soft matter*, 2014, **10**, 465-469.
11. P. Zhao, H. Liu, H. Deng, L. Xiao, C. Qin, Y. Du and X. Shi, *Colloids and Surfaces B: Biointerfaces*, 2014, **123**, 657-663.
12. X. Shi, H. Wu, Y. Li, X. Wei and Y. Du, *Journal of Biomedical Materials Research Part A*, 2013, **101**, 1373-1378.
13. L.-Q. Wu, K. Lee, X. Wang, D. S. English, W. Losert and G. F. Payne, *Langmuir*, 2005, **21**, 3641-3646.
14. K. D. Patel, T.-H. Kim, E.-J. Lee, C.-M. Han, J.-Y. Lee, R. K. Singh and H.-W. Kim, *ACS applied materials & interfaces*, 2014, **6**, 20214-20224.
15. P. Benito, M. Herrero, F. Labajos and V. Rives, *Applied Clay Science*, 2010, **48**, 218-227.
16. S. Y. Lee and J. H. Chang, *Biochemistry and Molecular Biology Reports*, 2011, **44**, 77-86.
17. S. Li, J. Li, C. J. Wang, Q. Wang, M. Z. Cader, J. Lu, D. G. Evans, X. Duan and D. O'Hare, *Journal of Materials Chemistry B*, 2013, **1**, 61-68.
18. L. Li, W. Gu, J. Chen, W. Chen and Z. P. Xu, *Biomaterials*, 2014, **35**, 3331-3339.
19. A. I. Khan, L. Lei, A. J. Norquist and D. O'Hare, *Chem. Commun.*, 2001, **22**, 2342-2343.

20. V. Ambrogi, G. Fardella, G. Grandolini and L. Perioli, *International Journal of Pharmaceutics*, 2001, **220**, 23-32.
21. L. Jin, D. He, Z. Li and M. Wei, *Materials Letters*, 2012, **77**, 67-70.
22. J. HyeonáLee, *Chemical Communications*, 2012, **48**, 5641-5643.
23. J. Liang, Y. Ma, S. Sims and L. Wu, *Journal of Materials Chemistry B*, 2015, **3**, 1281-1288.
24. A. Sinha, A. Chakraborty and N. R. Jana, *Acs Applied Materials & Interfaces*, 2014, **6**, 22183-22191.
25. F. Ding, X. Shi, Z. Jiang, L. Liu, J. Cai, Z. Li, S. Chen and Y. Du, *Journal of Materials Chemistry B*, 2013, **1**, 1729-1737.
26. H. Sereshti, S. Samadi and M. Karimi, *RSC Advances*, 2015, **5**, 9396-9404.
27. X. M. Li, Y. Y. Wang, J. M. Chen, Y. N. Wang, J. B. Ma and G. L. Wu, *Acs Applied Materials & Interfaces*, 2014, **6**, 3640-3647.
28. N. C. Fan, F. Y. Cheng, J. a. A. Ho and C. S. Yeh, *Angewandte Chemie International Edition*, 2012, **51**, 8806-8810.
29. F. Liu and M. W. Urban, *Progress in Polymer Science*, 2010, **35**, 3-23.
30. S. W. Choi, Y. Zhang and Y. Xia, *Angewandte Chemie International Edition*, 2010, **49**, 7904-7908.
31. I. Tokarev and S. Minko, *Soft Matter*, 2009, **5**, 511-524.
32. Z. P. Xu, G. S. Stevenson, C.-Q. Lu, G. Q. Lu, P. F. Bartlett and P. P. Gray, *Journal of the American Chemical Society*, 2006, **128**, 36-37.
33. Z. P. Xu and G. Q. Lu, *Chemistry of materials*, 2005, **17**, 1055-1062.
34. J. W. Boclair and P. S. Braterman, *Chemistry of Materials*, 1999, **11**, 298-302.
35. K.-C. Yang, Z. Qi, C.-C. Wu, Y. Shirouza, F.-H. Lin, G. Yanai and S. Sumi, *Biochemical and biophysical research communications*, 2010, **393**, 818-823.
36. Y.-J. Shyong, R.-F. Lin, H.-S. Soung, H.-H. Wei, Y.-S. Hsueh, K.-C. Chang and F.-H. Lin, *Journal of Materials Chemistry B*, 2015, **3**, 2331-2340.
37. S. Li, J. Li, C. J. Wang, Q. Wang, M. Z. Cader, J. Lu, D. G. Evans, X. Duan and D. O'Hare, *Journal of Materials Chemistry*, 2012, **1**, 61-68.
38. H. P. Corporation, *Spectroscopy*, 2007, **21**, 151-160.
39. C. J. Wang and D. O'Hare, *Journal of Materials Chemistry*, 2012, **22**, 21125-21130.
40. Q. Z. Yang, D. J. Sun, C. G. Zhang, X. J. Wang and W. A. Zhao, *Langmuir*, 2003, **19**, 5570-5574.
41. T. Akazawa and M. Kobayashi, *Journal of materials science letters*, 1996, **15**, 1319-1320.

SCHEMES AND FIGURES:

Scheme1. Illustration of the procedure for electrodeposition of multilayered chitosan/INS-LDHs hydrogel and stimuli-responsive insulin release

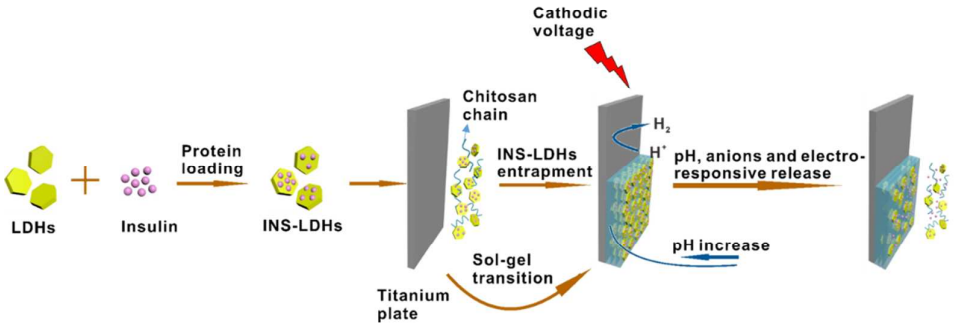

Table 1. The zeta potential of LDHs, insulin and INS-LDHs.

Sample	LDHs	insulin	INS-LDHs
Zeta potential(mV)	8.62	-19.43	-4.2

Figure 1. The SEM images (A) (B) and TEM images (C) (D) of Cl-LDHs.

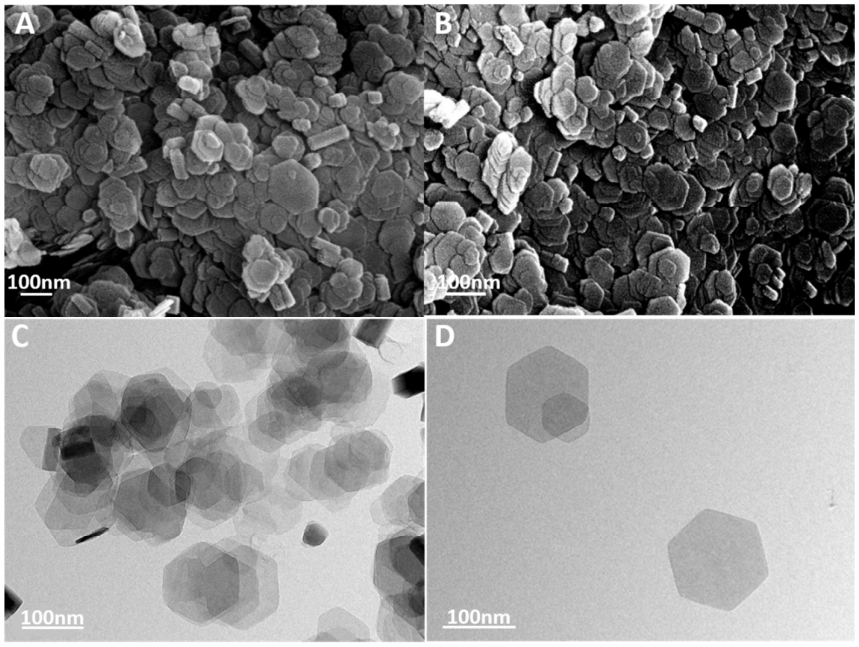

Figure 2. The EDS analysis of (A) LDHs, (B) INS-LDHs and the size distribution of (C) LDHs, (D) INS-LDHs.

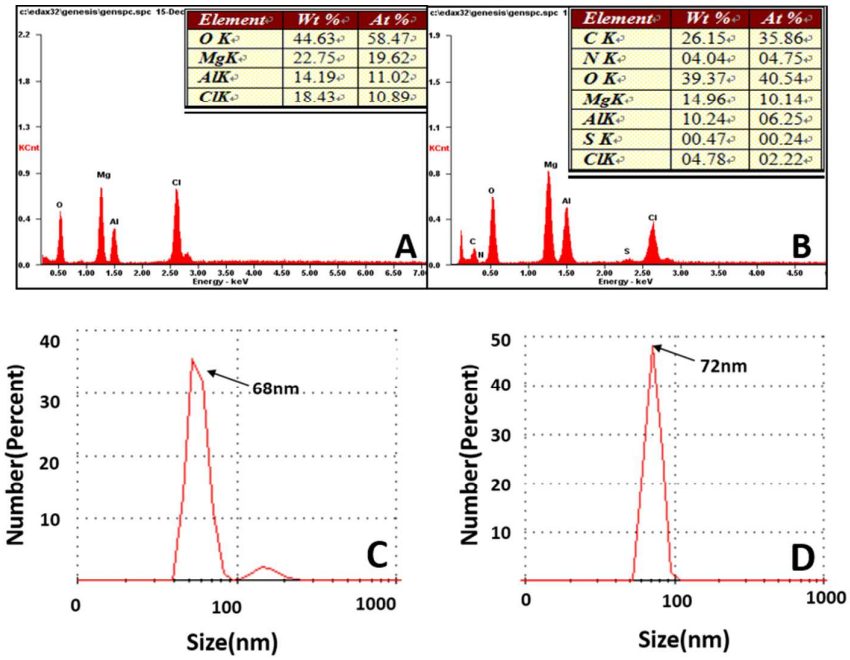

Figure 3. X-ray diffraction pattern (A), FT-IR spectra (B) and TG curves (C) of LDHs, INS-LDHs and insulin.

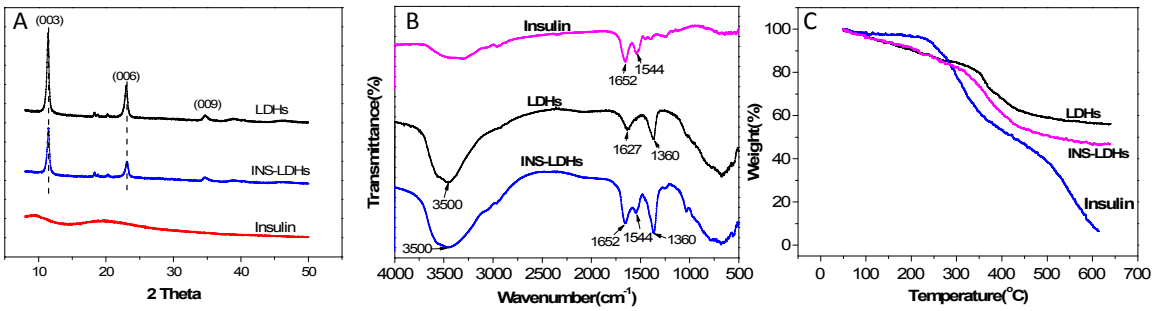

Figure 4. Cumulative release profiles of insulin from (A)INS-LDHs in 100 mM HPO_4^{2-},100 mM SO_4^{2-}, 100 mM CO_3^{2-}, 100 mM Cl^- or 100 mM NO_3^- at pH9 and (B) INS-LDHs in 10 mM, 5 mM or 1 mM phosphate buffer at pH7.4.

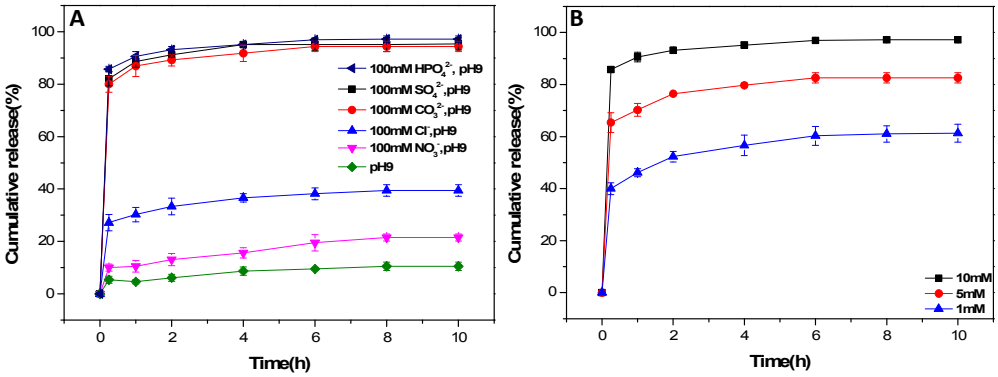

Figure 5. The optical and SEM images of pure chitosan gel (A, B, C) and chitosan/INS-LDHs gel (chitosan to LDHs mass ratio 1:1) (D, E, F). The optical images show the hydrogel on titanium plate after deposition. The SEM images show the cross-section of the hydrogel.

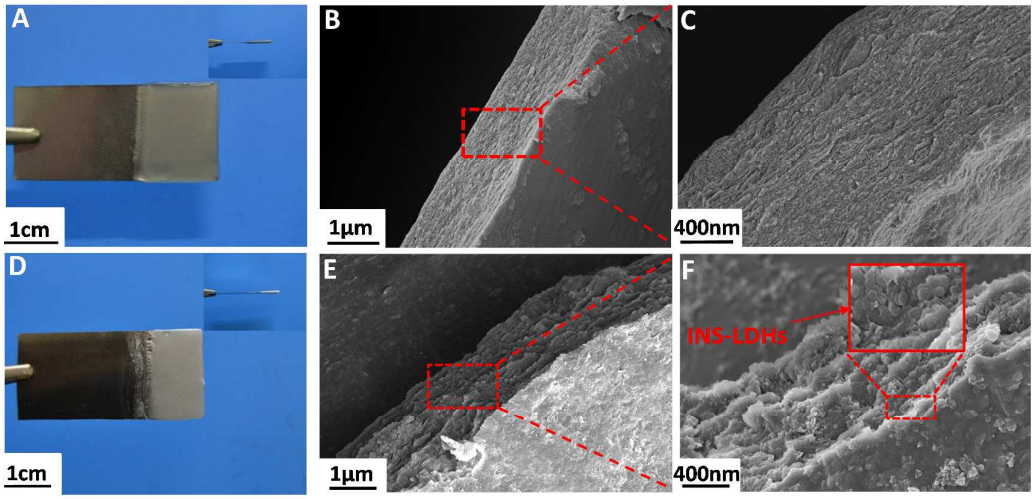

Figure 6. Cumulative release profiles of insulin from chitosan/INS-LDHs. (A) The release was performed by sequentially changing anions under different pHs (the dotted lines show the continuous release in 0.1 M NO_3^-); (B) The insulin release by biasing different voltages; (C) Step-wised release of insulin by adjusting the imposed on-off mode.

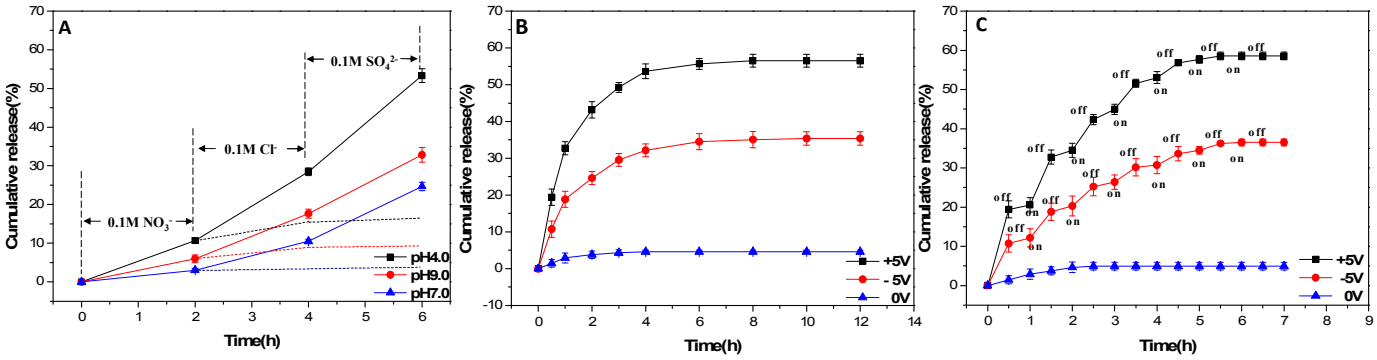

Graphical Abstract

Biomimetic brick-and-mortar structure was facilely constructed by co-deposition of chitosan and layered double hydroxides (LDHs). The release of entrapped insulin from the multilayered hydrogel could be tuned by the presence of pH, anion and electrical potential. (a single electrodeposition process to fabricate multilayered chitosan/layered double hydroxides (LDHs) hybrid hydrogel for stimuli responsive protein release.)